Published in final edited form as:
J Neurosci. 2011 January 5; 31(1): 78–88. doi:10.1523/JNEUROSCI.3542-10.2011.

Contexts for dopamine specification by calcium spike activity in the central nervous system

Norma A. Velázquez-Ulloa, **Nicholas C. Spitzer**, and **Davide Dulcis**
Neurobiology Section, Division of Biological Sciences and Center for Neural Circuits, Kavli Institute for Brain and Mind, University of California, San Diego, La Jolla, California 92093-0357.

Abstract

Calcium-dependent electrical activity plays a significant role in neurotransmitter specification at early stages of development. To test the hypothesis that activity-dependent differentiation depends on molecular context we investigated the development of dopaminergic neurons in the central nervous system of larval *Xenopus laevis*. We find that different dopaminergic nuclei respond to manipulation of this early electrical activity by ion channel misexpression with different increases and decreases in numbers of dopaminergic neurons. Focusing on the ventral suprachiasmatic nucleus and the spinal cord in order to gain insight into these differences, we identify distinct subpopulations of neurons that express characteristic combinations of GABA and NPY as co-transmitters and Lim1,2 and Nurr1 transcription factors. We demonstrate that the developmental state of neurons identified by their spatial location and expression of these molecular markers is correlated with characteristic spontaneous calcium spike activity. Different subpopulations of dopaminergic neurons respond differently to manipulation of this early electrical activity. Moreover, retinohypothalamic circuit activation of the ventral suprachiasmatic nucleus recruits expression of dopamine selectively in reserve pool neurons that already express GABA and neuropeptide Y. The results are consistent with the hypothesis that spontaneously active neurons expressing GABA are most susceptible to activity-dependent expression of dopamine both in the spinal cord and in the brain. Because loss of dopaminergic neurons plays a role in neurological disorders such as Parkinson's disease, understanding how subpopulations of neurons become dopaminergic may lead to protocols for differentiation of neurons *in vitro* to replace those that have been lost *in vivo*.

Keywords

tyrosine hydroxylase; neuronal differentiation; reserve pool neurons; neurotransmitters; GABA

INTRODUCTION

Calcium spike activity in embryonic and larval *Xenopus* regulates developmental specification of glutamate, GABA, glycine, and acetylcholine in neurons of the spinal cord (Borodinsky et al., 2004), dopamine in neurons of the ventral suprachiasmatic nucleus (VSC) of the hypothalamus (Dulcis and Spitzer, 2008) and serotonin in neurons of the raphe (Demarque and Spitzer, 2010). Neurons of the dopaminergic (DA) system are distinguishable by their connectivity and function, and include separate populations in the telencephalon, diencephalon, mesencephalon, and spinal cord (Smeets and Gonzalez, 2000). The DA system in *Xenopus* consists of the telencephalic olfactory bulb (OB), concerned

Corresponding author: Davide Dulcis. ddulcis@gmail.com.

with olfaction and kin recognition (Blaustein and Waldman, 1992); the diencephalic VSC and dorsolateral suprachiasmatic nuclei (DLSC) with roles in background adaptation (Ubink et al., 1998); and the mesencephalic posterior tuberculum (PT), equivalent to the substantia nigra and ventral tegmental area (VTA) in mammals, with roles in movement and reward (Marin et al., 1997; Endepols et al., 2004). The DA neurons of the spinal cord are cerebrospinal fluid (CSF)-contacting cells that extend an ascending axon toward the brain and are believed to respond to changes in the CSF (González et al., 1993; 1994; Heathcote and Chen, 1994; Vigh et al., 2004).

DA neurons are a heterogeneous population that expresses additional neurotransmitters. In adult *Xenopus*, neuronal subpopulations within the VSC co-express dopamine with GABA and/or NPY (de Rijk et al., 1992; Ubink et al., 1998; Tuinhof et al., 1994). In lamprey, dopamine and GABA co-localize in different DA nuclei (Barreiro-Iglesias et al., 2009). In rat, dopamine is co-expressed with GAD in the substantia nigra (Hedou et al., 2000) and in mouse dopamine is co-expressed with VGlut2 in the VTA (Dal Bo et al., 2008; Mendez et al., 2008). In addition, heterogeneity is observed in the transcription factors expressed by DA neurons. In *Xenopus*, Pax6 is expressed in the diencephalon and OB during development (Moreno et al., 2008). Pax6 has been associated with the development of diencephalic and OB DA neurons in mice (Vitalis et al., 2000; Mastick and Andrews, 2001; Kohwi et al., 2005) and zebrafish (Wullimann and Rink, 2001). Transcription factors Lim1 and Lim2 are expressed in the developing diencephalon in *Xenopus* (Moreno et al., 2004) and in the diencephalon of embryonic mouse brain (Mastick and Andrews, 2001). Nurr1 has been linked to development of mouse mesencephalic DA neurons, both in the VTA and substantia nigra (Zetterström et al., 1996, 1997; Jankovic et al., 2005; Ang, 2006) and zebrafish (Blin et al., 2008).

Since expression of dopamine is regulated by calcium spike activity in the VSC (Dulcis and Spitzer, 2008), we determined whether activity has a general role in dopamine specification across the nervous system. We find that DA neurons in different nuclei express different combinations of transmitters and transcription factors. Developing neurons exhibit distinct patterns of spontaneous calcium spike activity and show different changes in the number of DA neurons in response to manipulations of electrical activity. We conclude that activity-dependent dopamine specification is favored by spontaneous activity in GABAergic neurons.

MATERIALS AND METHODS

Animals

Xenopus laevis embryos were generated by *in vitro* fertilization and reared at 20–22°C. Animals were staged according to Nieuwkoop and Faber (1967). Because TH expression in the annulus of the VSC has been shown to be light-dependent (Dulcis and Spitzer, 2008) we standardized light exposure (12L/12D) and background (gray) in our experiments. All protocols were approved by the UCSD Institutional Animal Care and Use Committee.

Immunocytochemistry

Larvae were fixed in 4% paraformaldehyde and 0.025% glutaraldehyde phosphate-buffered saline (PBS) at pH 7.4 for 1–2 hr at 4°C. After fixation, larvae were rinsed twice in 1× Dulbecco calcium-magnesium-free phosphate-buffered saline (1×CMF-PBS, Sigma) and either cryoprotected in 30% sucrose in 1X CMF-PBS and embedded in optimal cutting temperature (OCT) medium (Tissue-Tek) for cryostat sections or rinsed and incubated in PBS-0.5% Triton (PBT) for 5 days for wholemounts. Cryostat 10 μm sections were taken following an anterior to posterior progression through the whole brain or through 600 to 800

μm of spinal cord starting 300–400 μm caudal to the eyes. For wholemounts, the brain and spinal cord of larvae were dissected after permeabilization in PBT. Sections or dissected wholemounts were permeabilized in PBT for 1 hr and then incubated in 1% fish gelatin (Sigma) in 1X CMF-PBS blocking solution for 1 hr at 20–22°C. One or two night incubation at 4°C with primary antibodies to tyrosine hydroxylase (TH; Imgenex), GABA (Chemicon), neuropeptide Y (NPY; Immunostar), Pax6 (Covance), Nurr1 (Santa Cruz Biotechnology), Lim3 (Millipore Bioscience Research Reagents), Lim1,2 and Isl1,2 (DSHB) was followed by incubation with fluorescently tagged secondary antibodies for 1 hr 30 min at 20–22°C. Sections were mounted with either Vectashield mounting medium with DAPI or Fluoromount (Southern Biotech); wholemounts were cleared in successive washes of 30%, 50%, and 80% glycerol and mounted in 80% glycerol. Immunoreactivity of singly stained sections was examined with a 20X water immersion objective on a Zeiss Axioscope, using a Xenon arc lamp attenuated by neutral density filters. Immunoreactivity of wholemounts and of double and triple stainings of sections was examined on a SP5 Leica confocal system; z-stacks were acquired to confirm co-localization and to generate through-series projections. For both microscopes, appropriate filter combinations for excitation and emission were used for Alexa 488, Alexa 594, Alexa 647, DAPI, FITC, or Cy3 fluorophores. Images were acquired and analyzed with either Axiovision or Leica Application Suite software. TH, the rate-limiting enzyme for dopamine synthesis, was used as a marker for dopamine. This enzyme has been shown to be a good marker for the DA nuclei and spinal cord neurons described in this paper, since TH colocalizes with other DA markers, including dopamine, DAT, and VMAT (Gonzalez et al., 1994; Dulcis and Spitzer, 2008), although TH has also been used as marker for noradrenaline in the locus coeruleus (Gonzalez et al., 1994).

Ion channel misexpression and light adaptation

DNA constructs for the human inward rectifying potassium channel (hKir2.1) and the rat voltage-gated sodium channel (rNa_v2a αβ) were gifts from E. Marban and W. Catterall. These constructs were subcloned, transcribed and expressed in all cells by injecting mRNA into both blastomeres at the two-cell stage along with a fluorescent tracer, Cascade Blue dextran (Invitrogen), to identify successfully injected embryos (Borodinsky, et al. 2004; Dulcis & Spitzer, 2008). Light-adaptation of stage 42 larvae was performed following the protocol described in Dulcis and Spitzer (2008).

Calcium imaging followed by immunostaining

To image DA neurons in the VSC we cut sections through the heads of larvae at the relevant stage and partially embedded these brain sections in low-melting point agarose (Promega) in a well filled with saline. This method led to stable preparations for imaging. To image DA neurons in the spinal cord, embryos were pinned ventral side up with 0.10-mm-diameter stainless-steel Austerlitz Minuten pins (Fine Science Tools) to the side of a well carved in the middle of a Sylgard-coated dish (Dow Corning). Incubation in 1–2% collagenase in saline (in mM: 116.6 NaCl, 0.67 KCl, 1.31 $MgSO_4$, 2.0 $CaCl_2$, 4.6 Tris; pH adjusted to 7.8 with HCl) for 15 min facilitated removal of tissue covering the ventral surface of the spinal cord, using forceps and tungsten needles. Brain sections and spinal cords were then rinsed in 2 mM calcium saline and incubated with Fluo-4 (5 μM Fluo4-AM/0.01% Pluronic Acid F-127/1% DMSO) for 1 hr at room temperature and gently washed in saline before imaging.

Calcium imaging of the brain was focused on the mid-ventral region of the sections, using the eyes, ventricle, and optic chiasm as landmarks to identify the VSC region. Calcium imaging of the spinal cord was carried out on a field of view covering the rostral to mid spinal cord regions, spanning 1,500 μm. The time-lapse imaging protocol lasted 30 min, acquiring images at 0.2 Hz on a BioRAD MRC-600 confocal microscope with a 20X water

immersion objective. Imaging was carried out at stages 39, 40, and 41 for the VSC and at stages 27, 28, and 29/30 for the spinal cord. Brain sections and spinal cords were immediately fixed with EDAC (Sigma-Aldrich, 40 mg/1 ml of 0.1X CMF-PBS) for 1 hr at room temperature to fix the calcium indicator Fluo-4 (Invitrogen; Dallwig and Deitmer, 2002), and then fixed for another hour in 4% paraformaldehyde + 0.025% glutaraldehyde at 4°C. Three 1 hr washes in 1X CMF-PBS were followed by permeabilization for 1– 2 nights in PBT. Brain sections and spinal cords were then incubated in blocking solution (1% fish gelatin in 1X CMF/PBS) for 12–24 hr. Brain sections were stained for TH, Lim1,2, and Nurr1; spinal cords were stained for TH and GABA. Incubation lasting 3–5 nights at 4°C was followed by 1 hr 30 min incubation with appropriate secondary antibodies and PBS washes. Immunopreparations were imaged on a Leica SP5 confocal by acquisition of 50–100 μm optical stacks. Projection of the Fluo-4 channel was used to match the calcium imaging movie to the staining. Changes in fluorescence in identified cells were analyzed by digitizing the time-lapse videos on Image J with the “Measure Stacks” plug-in by Bob Dougherty (Optinav, Inc). A region of interest (ROI) was drawn around the cell body, pixel intensity was measured across all frames of the movie, and intensity values were exported to Excel (Microsoft). Calcium spikes were identified on digitized traces as transients that increased in fluorescence 2× the baseline with a single frame rise time. We analyzed spike incidence (number of spiking neurons as a percent of the total number of neurons of that staining class) and frequency (number of spikes/30 min).

Statistical analysis

The incidence of immunostaining determined per brain region or spinal cord was used to calculate a mean ± SEM, using Excel (Figs. 1, 2, 4, 5, 8B & 10). To analyze changes in staining following perturbations of calcium spiking we determined the mean staining incidence, normalized it to control and calculated the mean ± SEM (Figs. 3 & 9). We determined the incidence and frequency of spontaneous calcium spiking for each subclass of neurons per brain slice or spinal cord and calculated the mean ± SEM (Fig. 7 & 8A). Statistical analyses were performed using the online software provided by BrightStat (Stricker, 2008). Comparisons between two groups were assessed by the non-parametric Mann Whitney U test. For comparisons of more than two groups the non-parametric Kruskal-Wallis test followed by Conover post-hoc test was used. Results are considered significant when $p<0.05$.

RESULTS

Sequential development of dopaminergic neurons in the brain and spinal cord

Wholemount preparations of brain and spinal cord stained with an antibody to tyrosine hydroxylase (TH), the rate-limiting enzyme for dopamine biosynthesis, established the time course of appearance of different DA nuclei as well as changes in relative position and shape of each nucleus throughout development (Fig. 1A,B). Our data confirm the caudal-to-rostral progression of differentiation of the DA phenotype, and illustrate a distinct temporal and spatial pattern for each nucleus (Gonzalez et al., 1994).

To obtain a more refined quantification of the temporal and spatial development of the DA system as a baseline for comparing changes following activity manipulations, we quantified the number of TH−immunoreactive (TH+) neuronal profiles in transverse sections through the brain (Fig. 1C,D). At stage 35, TH is detected in a few cells in the PT, which is the most caudal of the DA brain nuclei, and in the DLSC. At stage 40, TH is also expressed in the VSC and there is an incipient OB, the most rostral of the DA nuclei, composed of only a few TH+ cells. By stage 42 a cluster of TH+ cells is detected in the OB. All DA nuclei expand as more cells start expressing TH during further development.

TH+ neurons appear in the spinal cord at stage 28 (Heathcote and Chen, 1994). By stage 35, these cells are located on the ventral side of the spinal cord in two longitudinal rows. Developing spinal cord DA neurons undergo changes in size and position from the midline through stage 45 (Fig. 2B,C), a process that continues at later stages (Heathcote and Chen, 1994). Neuronal processes start developing rostrally at stage 40 (Fig. 2B, arrows), and by stage 42 axons extend anterolaterally along the longitudinal ventral axis. Confocal Z-stack reconstructions of dissected spinal cord wholemounts quantify the increase in number, decrease in size, and migration toward the midline during a 3-day period of development (Fig. 2D–F).

Specification of the dopaminergic phenotype is modulated by calcium spike activity to different extents in different regions

To test the activity-dependence of the DA phenotype, we overexpressed mRNA encoding hKir2.1 (Kir), an inward rectifier potassium channel, or rNa_v2a αβ (Na_v), a voltage-gated sodium channel; expression of these channels has been shown to decrease or increase calcium spike activity in the spinal cord and the brain (Borodinsky et al., 2004; Dulcis & Spitzer 2008) (Fig. 3A). The results of activity manipulations were quantified at stage 42, when all DA nuclei are present in control animals.

Na_v mRNA-injected embryos exhibited an increase in the number of TH+ neurons in the brain while Kir mRNA-injected embryos demonstrated a decrease compared to controls (Supplementary Fig. 1A). However, the level of the response varied among nuclei (Fig. 3B–E). Hyperactivity caused an increase in the number of TH+ neurons in the OB, DLSC, and VSC. The same nuclei responded to hypoactivity with a decrease in number of TH+ neurons. In contrast, while the number of TH+ profiles in the PT decreased with hypoactivity, hyperactivity yielded numbers that were not significantly different from control (Fig. 3E). Overexpression of Nav resulted in similar changes in calcium spike frequency in the VSC and PT (Supplementary Fig. 1B), suggesting that the PT is either less able to increase the number of TH cells in response to increased activity or that it requires a specific pattern of activity that is lost when activity is imposed by ion channel overexpression. Assessment of activity manipulations at earlier stages (37 and 40) did not reveal significant changes in the number of DA PT neurons, suggesting that the limited responsiveness of the PT observed at stage 42 is not due to developmental compensation (Supplementary Fig. 1C,D). Each brain nucleus responded to a different degree to the activity imposed by channel overexpression. In the spinal cord we also found an increase in the number of TH+ neurons following increased spike activity and a reduction in TH+ neurons following a decrease in spike activity compared to controls (Fig. 3F,G). Because the diencephalic VSC was the most responsive nucleus to activity manipulations in the brain and the spinal cord displayed the earliest onset of dopamine expression, we focused our study on the VSC and spinal cord to investigate further the context dependence of activity-dependent neurotransmitter specification.

Co-expression of neurotransmitters and transcription factors identifies subclasses of dopaminergic neurons in the VSC and spinal cord

To test the hypothesis that activity-dependent expression of TH/dopamine depends on the presence of additional molecular markers, such as neurotransmitters or transcription factors, we investigated the molecular heterogeneity of developing VSC and spinal cord neurons by immunocolocalizing TH with other molecular markers. Dopamine is co-expressed with GABA or NPY in the adult *Xenopus* suprachiasmatic nucleus (de Rijk et al., 1992; Ubink et al., 1998). A subpopulation of DA neurons of the VTA in mice and rat co-express VGlut2 (Kawano et al., 2006; Mendez et al., 2008, Hnasko et al., 2010). Dopamine is co-expressed in a subset of CSF-contacting GABA neurons of the adult lamprey spinal cord (Rodicio et

al., 2008), and dopamine and GABA colocalize to different degrees in various DA nuclei in its brain (Barreiro-Iglesias et al., 2009).

We studied co-localization of TH with additional neurotransmitters in the VSC at stages 40, 42, and 45, which span the onset of expression of TH in the core at stage 40, expression in the surrounding annulus by stage 42, and continued growth to stage 45. We found no co-localization of TH with VGlut2 at stages 40, 42 and 45 (data not shown) At stage 40 the DA VSC consists of a TH+ core region that is largely GABA− (Fig. 4A, graph). At this stage, neurons in the annular region are TH− but express NPY/GABA (not shown). By stage 42 a larger set of DA neurons has been recruited from the NPY/GABA cells in the annulus while the core retains a substantial TH+/GABA− composition (Fig. 4A). By stage 45, an additional TH+ subpopulation appears in an outer annulus that co-expresses NPY but is GABA−. This population persists in the adult suprachiasmatic nucleus (Ubink et al., 1998). In the spinal cord TH+ neurons are NPY− (Supplementary Fig. 2) and largely GABA+ from stage 29 to 45 (Fig. 5A,C).

Selective expression of transcription factors has been described for large regions of the brain, but the level of heterogeneity of transcription factor expression within individual DA nuclei in *Xenopus* during development has not received attention. We tested TH co-expression with Pax6, Nurr1, and Lim1,2, which have been implicated in DA differentiation in the developing diencephalon (Pax6, Lim1,2: Vitalis et al., 2000; Mastick and Andrews, 2001) and mesencephalon of mice (Nurr1: Zetterstrom et al., 1996, 1997; Ang, 2006). In addition, Nurr1 controls differentiation of DA neurons of the PT in zebrafish (Blin et al., 2008). Both Pax6 and Lim1,2 are expressed in the diencephalon throughout *Xenopus* development (Moreno et al., 2004, 2008).

To determine whether specific transcription factor expression is correlated with the different DA subclasses identified by their neurotransmitter expression pattern we co-stained neurons in the VSC for TH along with GABA and either Lim1,2, Nurr1 or Pax6. At stage 42, Nurr1+/TH+ cells expressing GABA are present in the outer annulus and the core is Nurr1− and Pax6− (Fig. 4B and Supplementary Fig. 3). Lim1,2 is expressed in neurons in the core and the annulus at this stage (Dulcis and Spitzer, 2008; Supplementary Fig. 3). The core contains two subclasses of neurons that express either TH and Lim1,2 or TH, Lim1,2 and GABA. Annular neurons expressing TH, GABA and NPY are Lim1,2+ but Nurr1− (Fig. 4C and 6A), while neurons in the outer annulus expressing TH, GABA and NPY are Nurr1+ but Lim1,2− (Fig. 4B and 6A). Thus, DA neuron subclasses defined by neurotransmitter co-expression do not correspond to expression domains of Lim1,2 or Nurr1. Each of these subpopulations –core, annulus, outer annulus- expresses specific combinations of neurotransmitters and transcription factors before they start expressing TH (Fig. 6A).

No transcription factors have yet been associated with specification of dopamine in the spinal cord. We tested the transcription factors linked to dopamine specification in the brain, but found no co-expression of TH with Lim 1,2, Nurr1 or Pax6. We also examined expression of Lim3, and Islet 1,2 that have been associated with neuronal differentiation of the ventral spinal cord (Appel et al., 1995), but neither of these markers were detected in TH + spinal neurons (Fig. 5B and 6B).

With this developmental picture of TH+ neurons in the VSC and spinal cord based on their temporal and spatial pattern of expression of neurotransmitters and transcription factors, we determined whether different DA nuclei and neuronal subclasses exhibit different frequencies of spontaneous calcium spike activity before the onset of TH expression and once TH is expressed.

Subclasses of dopaminergic neurons display distinct patterns of spontaneous calcium spike activity

The heterogeneity of subclasses observed within the VSC led us to hypothesize that individual subpopulations of DA neurons possess different endogenous calcium-mediated electrical activity. We imaged subclasses of DA cells within the VSC that express different combinations of molecular markers and the more homogeneous spinal cord DA neurons that are distantly located along the rostro-caudal axis of the CNS for comparison.

We focused our analysis of spontaneous calcium spike activity on a window of development that begins at a stage just prior to detection of TH expression (stage 27 for the spinal cord and stage 39 for the brain). We were not able to identify VSC core neurons at earlier stages because there is no Lim1,2+ cluster of cells 10 μm dorsal to the optic chiasm. This window of development ends at the latest stage at which spiking is detected (stage 30 in the spinal cord and stage 42 in the brain). In the VSC, Lim1,2+ (core + annulus) and Nurr1+ (outer annulus) DA precursors can be identified at stage 39 before the appearance of TH. At stage 40, some Lim1,2+ core neurons express TH, while both Lim1,2+ annulus and Nurr1+ outer annulus neurons are still TH−. By stage 41 TH starts to be expressed in the annular regions as well. Thus, we characterized calcium spike activity in neurons of the Lim1,2+ core, Lim1,2+ annulus, and the Nurr1+ outer annulus of the VSC before and after they acquired TH.

We found that the activity of core and annular neurons is distinct: core neurons did not exhibit spontaneous calcium activity, either before or after expressing TH (Lim1,2+ or TH+/Lim1,2+), although they can generate spikes in response to overexpression of Na_v (Dulcis and Spitzer, 2008). On the other hand, annular neurons exhibited robust activity, the incidence and frequency of which changed during development. At stage 39 TH− cells expressing either Lim1,2 or Nurr1 have a similar incidence and frequency of spiking. However, their activity patterns diverge by stage 41, with a lower spiking frequency for TH−/Nurr1+ cells compared to TH−/Lim1,2+ cells. As annular cells now acquire the TH phenotype, their activity patterns are correlated with the transcription factor they express. TH+/Lim1,2+ neurons no longer exhibit spiking, while TH+/Nurr1+ cells are active at a level similar to that of TH−/Nurr1+ cells at stage 41 (Fig. 7A,B).

In the spinal cord we examined endogenous calcium activity of DA neurons at stages 27, 28, and 29/30, which encompass the period during which GABAergic ventral midline neurons acquire the additional DA phenotype. Calcium spike frequency increases in the GABA+/TH+ population at stage 28 (Fig. 8A). The spike incidence of the GABA+/TH+ cells remains constant during this period. The proportion of TH− and TH+ cells within the GABA+ population on the ventral surface of the spinal cord reverses during this period of development, as the GABA+/TH− population decreases and the GABA+/TH+ population increases (Fig. 8B), coincident with increased spike frequency at stage 28.

These results are consistent with the hypothesis that subclasses of TH− precursors and TH+ cells identified by different molecular markers and by their spatial location display different patterns of calcium spike activity at the same time point during development. The results also indicate that single molecular markers of DA neuron precursors are not always correlated with specific patterns of activity. Cells that express Lim1,2 can be active or not, depending on whether they are located in the core region or annular region of the VSC. Moreover, cells that express different transcription factors (Nurr1 or Lim1,2), but are located in the annular regions initially display similar incidence and frequency of calcium spikes.

Dopaminergic subclasses display different responsiveness to activity manipulation

We next characterized the expansion of the DA phenotype in the VSC and spinal cord following an increase in activity by overexpression of Na_v channels. The neurons in both regions are responsive to an increase in activity, but the induction of neurotransmitter specification is different in each region.

In the VSC, increased activity leads to expression of Pax6 that is not normally present in controls (Dulcis and Spitzer, 2008). Most of the newly TH+ reserve pool neurons induced by increased activity are recruited from this ectopic Pax6+/Lim1,2+ neuronal population. We focused on the core and annular region that have been previously studied following manipulations of activity (Dulcis and Spitzer, 2008). Following Na_v overexpression we found that the increase in the number of TH+/Lim1,2+ neurons in the annular region is larger than the increase in the number of neurons that are TH+/Lim1,2+ in the core (Fig. 9A). Annular reserve pool neurons, which display endogenous calcium spike activity during normal developmental acquisition of the TH phenotype, are more responsive to activity manipulation than neurons in the core. While the expansion of the TH phenotype occurs within the available Lim1,2+ cell pool, the total number of Lim1,2+ neurons in the core and annulus does not change following activity manipulation (Dulcis and Spitzer, 2008); thus it is unlikely that neurogenesis contributes to these results.

Expansion of the TH phenotype in the spinal cord occurs within the GABA+ cells localized in ventral longitudinal rows and adjacent to the central canal. In controls, TH+/GABA+ cells are distributed along the spinal cord and only single cell profiles are seen in 10 μm transverse sections. The number of ventral GABA+ cells is not significantly altered by increased activity, but Na_v overexpression causes more of these GABA+ cells to acquire the TH phenotype, increasing the occurrence of clusters of TH+/GABA+ cells in transverse sections (Fig. 9B). The limited induction of TH expression within these cells suggests that ventral spinal GABA+ cells possess a selective responsiveness to activity, and that a subset of these GABA+ cells serves as reserve pool neurons for additional TH expression in the spinal cord.

Circuit activity recruits TH expression selectively in GABAergic annular neurons of the VSC

To understand the physiological relevance of the molecular and spatio-temporal calcium spike diversity identified within the DA system, including the different responsiveness of TH+ neuronal subclasses to activity manipulations, we tested the effect on transmitter specification of activity triggered by sensory circuit stimulation. In contrast to molecular overexpression of ion channels, a 2 hr period of white light illumination on a white background affects the activity of neurons without affecting the endogenous diversity of developmental calcium spike activity at earlier stages. Annular NPY neurons of the VSC acquire the DA phenotype following calcium-dependent activation of the retinohypothalamic projection by light (Dulcis and Spitzer, 2008). We found that NPY+ neurons acquiring TH in light-adapted larvae are GABA+ (Fig. 10) as well as Lim1,2+ (Dulcis and Spitzer, 2008); NPY+ neurons lacking GABA were not recruited to express TH in response to sensory stimulation. Dark adaptation on a black background causes a reduction in number of TH+ and TH+/NPY+/GABA+ neurons in the annulus compared to control (Fig. 10C). GABA expression detected in NPY+ annular neurons before TH specification persists after circuit activation and DA induction, leading to co-expression of three inhibitory transmitters (GABA, NPY, and dopamine). These experiments suggest that VSC neurons expressing GABA serve as a reserve pool of neurons that can acquire an additional neurotransmitter - dopamine. Our results show that not all of the potentially available reserve pool neurons are recruited by activity for dopamine specification in a

circuit-dependent fashion. Among the NPY+ annular neurons, only those co-expressing GABA were selected.

DISCUSSION

Calcium spike activity is required for transmitter specification in neurons of the spinal cord and VSC of *Xenopus* embryos and larvae (Borodinsky et al., 2004; Dulcis and Spitzer, 2008). Here we extend these results, showing that calcium spikes modulate dopamine specification in multiple regions of the CNS and in a heterogeneous population of DA cells that display additional neurotransmitters and particular transcription factors. Specification of another monoamine, serotonin, is also activity-dependent in the raphe (Demarque and Spitzer, 2010). These studies demonstrate that calcium spike activity-dependent transmitter specification is a general process across the *Xenopus* nervous system and for a variety of neurotransmitters, consistent with developmental activity-dependent regulation of dopamine expression in rat primary sensory neurons (Brosenitsch et al., 1998, 2002) and acetylcholine in mouse hypothalamic neurons (Liu et al., 2008).

Classifying dopaminergic neurons in space and time

Dopamine expression appears in the *Xenopus* CNS in a distinct spatial and temporal pattern, following a caudal-to-rostral progression (Gonzalez et al, 1994) as observed in zebrafish and lamprey (McLean and Fetcho, 2004; Abalo et al., 2005). Expression of a particular transcription factor or neurotransmitter provides a basis for classifying neurons. However, cell identity is a complex combinatorial signature that includes co-expression of multiple transmitters and transcription factors in subsets of neuronal populations (Hökfelt, 1991; Trudeau and Gutierrez, 2007). Developing DA neurons in the VSC are heterogeneous, with subpopulations that display specific combinations of GABA, NPY, Lim1,2, and Nurr1. Each subpopulation can also be identified by its stereotypic anatomical location within each nucleus and the stage of development at which this subpopulation appears.

The additional subpopulations that appear during normal development are most likely postmitotic cells acquiring their final neurotransmitter phenotypes and not newly generated neurons. The first wave of neurogenesis in *Xenopus* occurs during gastrulation, with the final mitosis occurring between stages 13–16 (Lamborghini, 1980; Hartenstein, 1989). The second wave of neurogenesis begins at stage 46 in the spinal cord and stage 48 in the brain (Schlosser et al., 2002; Wullimann et al., 2005), after the stages covered in the present study (stages 29 to 45). The DA subpopulations within the VSC are molecularly distinct prior to expression of the DA phenotype, and not simply members of the same neuronal population at different stages of differentiation.

Interestingly, VSC neurons can be clustered into two groups expressing different transcription factors, Lim1,2 and Nurr1. Nurr1 expression has been implicated in the survival and differentiation of mesencephalic DA neurons in mice (Zetterstrom et al., 1997) and zebrafish (Blin et al., 2008). Here we report expression of Nurr1 in DA neurons in the diencephalon as well. Future work will identify additional transcription factors expressed in these neurons.

In the spinal cord dopamine is expressed in a subset of the GABAergic CSF-contacting Kolmer-Agduhr (KA) neurons (Dale et al. 1987a,b; Binor and Heathcote, 2001). Dopaminergic and GABAergic KA cells were thought to be different populations. Here we show that some of these GABAergic cells co-express TH. Developmentally, GABA expression precedes TH expression. GABA is first detected in the ventral spinal cord at stage 25 (Dale et al., 1987b), while TH expression starts at stage 28 (Heathcote and Chen, 1994).

It is becoming clear that the differentiation of neuronal populations thought to be homogeneous for neurotransmitter expression occurs in a complex spatio-temporal pattern. The DA system exemplifies a highly heterogeneous population of neurons, all of which share the expression of the transmitter dopamine yet diverge in their expression of additional markers. Brain nuclei previously described as cell clusters sharing the same function actually include subclasses of neurons with distinct endogenous calcium spike activity and responsiveness to activity that may enable accomplishment of the myriad tasks that a single brain nucleus controls.

Relationship of transmitters and transcription factors to endogenous patterns of excitability

Given the diversity of molecular markers within the DA system, we tested the hypothesis that developing DA neurons with different molecular markers display different patterns of calcium spike activity. VSC neurons exhibit different patterns of calcium spike incidence and frequency that are correlated with location within the nucleus and the transcription factor(s) they express. Neurons in the core expressing either Lim1,2, or TH/Lim1,2 did not exhibit calcium spike activity between stage 39 and 41. In contrast, Lim1,2+ and Nurr1+ annular and outer annular cells exhibit spiking that diverges during development. Acquisition of TH in GABA+ cells is associated with a decrease in frequency of calcium spiking. Examination of spinal cord neurons identified as GABA+/TH− or GABA+/TH+ revealed that each population has different frequencies of spiking that change during development and cell differentiation. A peak in spiking frequency is observed at the time that spinal cord GABA+ cells are acquiring TH. Thus DA neurons and precursors identified by specific molecular markers and located in different regions of the CNS display particular patterns of spiking during the stages in which TH is acquired.

Dopamine and GABA: co-expression partners?

Dopamine and GABA appear to be preferred co-expression partners. *Tottering* (Hess and Wilson, 1991; Fletcher et al, 1996) and *leaner* (Abbott et al, 1996; Austin et al, 1992) mice with calcium channel mutations and neurological abnormalities including seizures and ataxia exhibit ectopic TH expression in a subset of normally GABAergic cerebellar Purkinje cells. TH is transiently expressed in Purkinje cells during normal development; in contrast, co-expression in these mutant mice persists throughout adulthood, suggesting that GABA+ Purkinje cell clusters responding to altered activity have a predisposition to acquire the DA phenotype by increasing TH co-expression. Under normal conditions, only a few intrinsic putatively GABAergic neurons in the rodent striatum co-express dopamine (Tashiro et al., 1989; Mao et al., 2001). When the substantia nigra is damaged in mice, striatal GABA+/TH + neurons increase in number (Lopez-Real et al., 2003). Similarly, the normal monkey and human striatum, which contain more DA neurons than that of rodents (Dubach et al., 1987; Palfi et al., 2002), respond to massive striatal DA denervation by recruiting GABAergic striatal neurons to express TH (Tande' et al., 2006; Hout and Parent, 2007). These GABAergic neurons that can be induced to express TH appear to correspond to the reserve pool neurons described for the VSC and spinal cord.

Dopamine is co-expressed with GABA in the olfactory bulb of mice (Hack et al., 2005), in specific subpopulations of the DA system in adult lamprey (Rodicio et al., 2008; Barreiro-Iglesias et al., 2009) and in the adult suprachiasmatic nucleus as well as the developing VSC and spinal cord in *Xenopus* (Ubink et al., 1998; this study). In white-adapted *Xenopus laevis* larvae, NPY+ annular reserve pool neurons of the VSC that are recruited to co-express dopamine (Dulcis and Spitzer, 2008) belong to a GABAergic neuronal population surrounding the core neurons.

The DA phenotype often appears to be recruited by altered circuit activity in GABAergic neurons of brain regions that have been shown to be capable of spontaneously expressing dopamine either transiently during development or persistently throughout adulthood. These observations suggest the existence of activity-dependent regulatory components controlling dopamine expression in reserve pool GABAergic neurons. Two regulatory elements in the TH promoter, the TH−Fat Specific Element (TH−FSE) that binds the Fos-Jun complex and the cAMP Response Element (CRE) that binds CREB, have been implicated in regulating TH gene transcription (Ghee et al., 1998). Since expression of both CREB (Hardingham et al., 1997) and Fos-Jun (Xia et al., 1996) transcription factors is activity-dependent, they may be links through which activity triggers dopamine specification in GABAergic neurons. Linkage to GABAergic neurons could also be provided by GABA spillover (Scanziani, 2000) that can activate $GABA_B$ receptors on GABAergic neurons (Liang et al., 2000); direct interaction of $GABA_B$ receptors with CREB2 and ATFx transcription factors (White et al., 2000) would provide a potential route for dopamine specification.

Conclusions

We have shown that dopamine specification is activity-dependent to different extents across the DA nervous system. Specific co-transmitters and transcription factors identify subgroups of DA neurons that display distinct patterns of calcium spike activity during development. GABA and spontaneous activity appear to be common factors in DA neurons responsive to calcium spike activity. A model emerges in which electrical activity regulates transmitter specification by mediating expression or activation of transcription factors. Lmx1b and Tlx3 are regulated by calcium spike activity, and changes in their expression and activation lead to changes in transmitter expression (Demarque and Spitzer, 2010; Marek et al., 2010). The results support the hypothesis that the molecular context provided by specific combinations of co-transmitters and transcription factors regulates calcium spike activity and dopamine specification. Calcium spikes may also act as an upstream signal to recruit specific transcription factors that activate terminal selector genes to achieve spatio-temporal specification of dopamine expression in reserve pool neurons (Flames and Hobert, 2009). Understanding how transcription factors and electrical activity participate together in differentiation of neuronal precursors into mature DA neurons could help improve clinical treatments such as stem cell transplantation. Specific patterns of calcium activity may be important in regulating the expression of combinations of transcription factors and transmitters that subclasses of DA neurons display *in vivo*.

Supplementary Material

Refer to Web version on PubMed Central for supplementary material.

Acknowledgments

This research was supported by National Institutes of Health Grant R01NS15918 to N.C.S. and a CONACYT-UC MEXUS fellowship to N.A.V.U. We thank members of our laboratory for helpful discussions and technical assistance; Darwin Berg, and Yimin Zou for comments on the manuscript; and A. de la Torre and I. Hsieh for technical support.

REFERENCES

Abalo XM, Villar-Cheda B, Anadón R, Rodicio MC. Development of the dopamine-immunoreactive system in the central nervous system of the sea lamprey. Brain Research Bulletin. 2005; 66:560–564. [PubMed: 16144650]

Abbott LC, Isaacs KR, Heckroth JA. Co-localization of tyrosine hydroxylase and zebrin II immunoreactivities in Purkinje cells of the mutant mice, tottering and tottering/leaner. Neuroscience. 1996; 71:461–475. [PubMed: 9053800]

Ang SL. Transcriptional control of midbrain dopaminergic neuron development. Development. 2006; 133:3499–3506. [PubMed: 16899537]

Austin MC, Schultzberg M, Abbott LC, Montpied P, Evers JR, Paul SM, Crawley JN. Expression of tyrosine hydroxylase in cerebellar Purkinje neurons of the mutant tottering and leaner mouse. Molecular Brain Research. 1992; 15:227–240. [PubMed: 1279353]

Appel B, Korzh V, Glasgow E, Thor S, Edlund T, Dawid IB, Eisen JS. Motoneuron fate specification revealed by patterened LIM homeobox gene expression in embryonic zebrafish. Development. 1995; 121:4114–4125.

Barreiro-Iglesias A, Villar-Cerviño V, Anadón R, Rodicio MC. Dopamine and γ-aminobutyric acid are colocalized in restricted groups of neurons in the sea lamprey brain: insights into early evolution of neurotransmitter colocalization in vertebrates. Journal of Anatomy. 2009; 215:601–610. [PubMed: 19840024]

Binor E, Heathcote RD. Development of GABA-immunoreactive neuron patterning in the spinal cord. Journal of Comparative Neurology. 2001; 438:1–11. [PubMed: 11503149]

Blaustein AR, Waldman B. Kin recognition in anuran amphibians. Animal Behavior. 1992; 44:207–221.

Blin M, Norton W, Bally-Cuif L, Vernier P. NR4A2 controls the differentiation of selective dopaminergic nuclei in the zebrafish brain. Molecular and Cellular Neuroscience. 2008; 39:592–604. [PubMed: 18822380]

Borodinsky LN, Root CM, Cronin JA, Sann SB, Gu X, Spitzer NC. Activity-dependent homeostatic specification of transmitter expression in embryonic neurons. Nature. 2004; 429:523–530. [PubMed: 15175743]

Brosenitsch TA, Salgado-Commissariat D, Kunze DL, Katz DM. A role for L-type calcium channels in developmental regulation of transmitter phenotype in primary sensory neurons. Journal of Neuroscience. 1998; 18:1047–1055. [PubMed: 9437025]

Brosenitsch TA, Katz DM. Expression of Phox2 transcription factors and induction of the dopaminergic phenotype in primary sensory neurons. Molecular and Cellular Neuroscience. 2002; 20:447–457. [PubMed: 12139921]

De Rink EPCT, van Strien FJC, Roubos EW. Demonstration of coexisting catecholamine (dopamine), amino acid (GABA), and peptide (NPY) involved in inhibition of melanotrope cell activity in *Xenopus laevis*: A quantitative ultrastructural, freeze-substitution immunocytochemical study. Journal of Neuroscience. 1992; 12:864–871. [PubMed: 1312137]

Dal Bo G, Bérubé-Carrière N, Mendez JA, Leo D, Riad M, Descarries L, Lévesque D, Trudeau LE. Enhanced glutamatergic phenotype of mesencephalic dopamine neurons after neonatal 6-hydroxydopamine lesion. Neuroscience. 2008; 156:59–70. [PubMed: 18706980]

Dale N, Roberts A, Ottersen OP, Storm-Mathisen J. The morphology and distribution of 'Kolmer-Agduhr cells', a class of cerebrospinal-fluid-contacting neurons revealed in the frog embryo spinal cord by GABA immunocytochemistry. Proceedings of the Royal Society of London. Series B, Biological Sciences. 1987; 232:193–203.

Dale N, Roberts A, Ottersen OP, Storm-Mathisen J. The development of a population of spinal cord neurons and their axonal projections revealed by GABA immunocytochemistry in frog embryos. Proceedings of the Royal Society of London. Series B, Biological Sciences. 1987; 232:205–215.

Demarque M, Spitzer NC. Activity-dependent expression of Lmx1b regulates specification of serotonergic neurons modulating swimming behavior. Neuron. 2010; 67:321–334. [PubMed: 20670838]

Dubach M, Schmidt R, Kunkel D, Bowden DM, Martin R, German DC. Primate neostratial neurons containing tyrosine hydroxylase: immunohistochemical evidence. Neuroscience Letters. 1987; 75:205–210. [PubMed: 2883616]

Dulcis D, Spitzer NC. Illumination controls differentiation of dopamine neurons regulating behavior. Nature. 2008; 456:195–201. [PubMed: 19005547]

Endepols H, Schul J, Gerhardt HC, Walkowiak W. 6-hydroxydopamine lesions in anuran amphibians: a new model system for Parkinson's disease? Journal of Neurobiology. 2004; 60:395–410. [PubMed: 15307145]

Fletcher CF, Lutz CM, O'Sullivan TN, Shaughnessy JD, Hawkes R Jr, Frankel WN, Copeland NG, Jenkins NA. Absence epilepsy in tottering mutant mice is associated with calcium channel defects. Cell. 1996; 87:607–617. [PubMed: 8929530]

Flames N, Hobert O. Gene regulatory logic of dopamine neuron differentiation. Nature. 2009; 458:885–889. [PubMed: 19287374]

Ghee M, Baker H, Miller JC, Ziff EB. AP-1, CREB and CBP transcription factors differentially regulate the tyrosine hydroxylase gene. Molecular Bain Research. 1998; 55:101–114.

Gonzalez A, Tuinhof R, Smeets WJAJ. Distribution of tyrosine hydroxylase and dopamine immunoreactivities in the brain of the South African clawed frog *Xenopus laevis*. Anatomical Embryology. 1993; 187:193–201.

Gonzalez A, Marin O, Tuinhof R, Smeets WJAJ. Ontogeny of catecholamine systems in the central nervous system of anuran amphibians: an immunohistochemical study with antibodies against tyrosine hydroxylase and dopamine. Journal of Comparative Neurology. 1994; 346:63–79. [PubMed: 7962712]

Hack MA, Saghatelyan A, de Chevigny A, Pfeifer A, Ashery-Padan R, Lledo PM, Götz M. Neuronal fate determinants of adult olfactory bulb neurogenesis. Nature Neuroscience. 2005; 8:865–872.

Hardingham GE, Chawla S, Johnson CM, Bading H. Distinct functions of nuclear and cytoplasmic calcium in the control of gene expression. Nature. 1997; 385:260–265. [PubMed: 9000075]

Hartenstein V. Early neurogenesis in *Xenopus*: the spatio-temporal pattern of proliferation and cell lineages in the embryonic spinal cord. Neuron. 1989; 3:399–411. [PubMed: 2642003]

Heathcote RD, Chen A. Morphogenesis of catecholaminergic interneurons in the frog spinal cord. Journal of Comparative Neurology. 1994; 342:57–68. [PubMed: 7911478]

Hedou G, Chasserot-Golaz S, Kemmel V, Gobaille S, Roussel G, Artault JC, Andriamampandry C, Aunis D, Maitre M. Immunohistochemical studies of the localization of neurons containing the enzyme that synthesized dopamine, GABA, or gamma-hydroxybutyrate in the rat substantia nigra and striatum. Journal of Comparative Neurology. 2000; 426:549–560. [PubMed: 11027398]

Hess EJ, Wilson MC. Tottering and leaner mutations perturb transient developmental expression of tyrosine hydroxylase in embryologically distinct Purkinje cells. Neuron. 1991; 6:123–132. [PubMed: 1670919]

Hnasko TS, Chuhma N, Zhang H, Goh GY, Sulzer D, Palmiter RD, Rayport S, Edwards RH. Vesicular glutamate transport promotes dopamine storage and glutamate corelease in vivo. Neuron. 2010; 65:643–656. [PubMed: 20223200]

Hökfelt T. Neuropeptides in perspective: the last ten years. Neuron. 1991; 7:867–879. [PubMed: 1684901]

Hout and Parent. Dopaminergic neurons intrinsic to the striatum. Journal of Neurochemistry. 2007; 101:1441–1447. [PubMed: 17286588]

Jankovik J, Chen S, Le WD. The role of Nurr1 in the development of dopaminergic neurons and Parkinson's disease. Progress in Neurobiology. 2005; 77:128–138. [PubMed: 16243425]

Kawano M, Kawasaki A, Sakata-Haga H, Fukui Y, Kawano H, Nogami H, Hisano S. Particular subpopulations of midbrain and hypothalamic dopamine neurons express vesicular glutamate transporter 2 in the rat brain. Journal of Comparative Neurology. 2006; 498:581–592. [PubMed: 16917821]

Kohwi M, Osumi N, Rubenstein JLR, Alvarez-Buylla A. Pax6 is required for making specific subpopulations of granule and periglomerular neurons in the olfactory bulb. Journal of Neuroscience. 2005; 25:6997–7003. [PubMed: 16049175]

Lamborghini JE. Rohon-beard cells and other large neurons in *Xenopus* embryos originate during gastrulation. Journal of Comparative Neurology. 1980; 189:323–333. [PubMed: 7364967]

Liang F, Hatanaka Y, Saito H, Yamamori T, Hashikawa T. Differential expression of γ-aminobutyric acid type B receptor-1a and -1b mRNA variants in GABA and non-GABAergic neurons of the rat brain. Journal of Comparative Neurology. 2000; 416:475–495. [PubMed: 10660879]

Liu X, Popescu IR, Denisova JV, Neve RL, Corriveau RA, Belousov AB. Regulation of cholinergic phenotype in developing neurons. Journal of Neurophysiology. 2008; 99:2443–2455. [PubMed: 18322006]

Lopez-Real A, Pallares JR, Guerra MJ, Labandira-Garcia JL. Localization and functional significance of striatal neurons immunoreactive to aromatic L-amino acid decarboxylase or tyrosine hydroxylase in rat Parkinsonian models. Brain Research. 2003; 969:135–146. [PubMed: 12676374]

Mao LM, Lau YS, Petroske E, Wang JQ. Profound astrogenesis in the striatum of adult mice following nigrostriatal dopaminergic lesion by repeated MPTP administration. Developmental Brain Research. 2001; 131:57–65. [PubMed: 11718836]

Marek KW, Kurtz LM, Spitzer NC. cJun integrates calcium activity and *tlx3* expression to regulate neurotransmitter specification. Nature Neuroscience. 2010; 13:944–950.

McLean DL, Fetcho JR. Ontogeny and innervation patterns of dopaminergic, noradrenergic and serotonergic neurons in larval zebrafish. Journal of Comparative Neurology. 2004; 480:38–56. [PubMed: 15515022]

Marin O, Smeets WJAJ, Gonzalez A. Basal ganglia organization in amphibians: development of striatal and nucleus accumbens connections with emphasis on the catecholaminergic inputs. Journal of Comparative Neurology. 1997; 383:349–369. [PubMed: 9205046]

Mastick GS, Andrews GL. Pax6 regulates the identity of embryonic diencephalic neurons. Molecular and Cellular Neuroscience. 2001; 17:190–207. [PubMed: 11161479]

Mendez JA, Bourque MJ, Dal Bo G, Bourdeau ML, Danik M, Williams S, Lacaille JC, Trudeau LE. Journal of Neuroscience. 2008; 28:6309–6318. [PubMed: 18562601]

Moreno N, Bachy I, Retaux S, Gonzalez A. LIM-homeodomain genes as developmental and adult genetic markers of *Xenopus* forebrain functional subdivisions. Journal of Comparative Neurology. 2004; 472:52–72. [PubMed: 15024752]

Moreno N, Retaux S, Gonzalez A. Spatio-temporal expression of Pax6 in *Xenopus* forebrain. Brain Research. 2008; 1239:92–99. [PubMed: 18786519]

Nieuwkoop, PD.; Faber, J. Normal table of *Xenopus laevis* (Daudin). Ed 2. North Holland: Amsterdam;

Palfi S, Leventhal L, Chu Y, Ma SY, Emborg M, Bakay R, Déglon N, Hantraye P, Aebischer P, Kordower JH. Lentivirally delivered glial cell line-derived neurotrophic factor increases the number of striatal dopaminergic neurons in primate models of nigrostriatal degeneration. Journal of Neuroscience. 2002; 22:4942–4954. [PubMed: 12077191]

Rodicio MC, Villar-Cerviño V, Barreiro-Iglesias A, Anadón R. Colocalization of dopamine and GABA in spinal cord neurones in the sea lamprey. Brain Research Bulletin. 2008; 76:45–49. [PubMed: 18395609]

Scanziani M. GABA spillover activates postsynaptic $GABA_B$ receptors to control rhythmic hippocampal activity. Neuron. 2000; 25:673–681. [PubMed: 10774734]

Scholsser G, Koyano-Nakagawa N, Kintner C. Thyroid hormone promotes neurogenesis in the *Xenopus* spinal cord. Developmental dynamics. 2002; 225:485–498. [PubMed: 12454925]

Smeets WJAJ, Gonzalez A. Catecholamine systems in the brain of vertebrates: new perspectives through a comparative approach. Brain Research Reviews. 2000; 33:308–379. [PubMed: 11011071]

Stricker D. BrightStat.com: Free statistics online. Computer Methods and Programs in Biomedicine. 2008; 92:135–143. (abstract). [PubMed: 18653259]

Tandé D, Höglinger G, Debeir T, Freundlieb N, Hirsch EC, François C. New striatal dopamine neurons in MPTP-treated macaques result from a phenotypic shift and not neurogenesis. Brain. 2006; 129:1194–1200. [PubMed: 16481374]

Tashiro Y, Sugimoto T, Hattori T, Uemura Y, Nagatsu I, Kikuchi H, Mizuno N. Tyrosine hydroxylase-like immunoreactive neurons in the striatum of the rat. Neuroscience Letters. 1989; 97:6–10. [PubMed: 2563908]

Trudeau LE, Gutiérrez R. On cotransmission and neurotransmitter phenotype plasticity. Molecular Interventions. 2007; 7(3):138–146. [PubMed: 17609520]

Tuinhof R, Gonzalez A, Smeets WJAJ, Roubos EW. Neuropeptide Y in the developing and adult brain of the South African clawed toad Xenopus laevis. Journal of Chemical Neuroanatomy. 1994; 7:271–283. [PubMed: 7873097]

Ubink R, Tuinhof R, Roubos EW. Identification of suprachiasmatic-inhibiting neurons in *Xenopus laevis*: a confocal laser-scanning microscopy study. Journal of Comparative Neurology. 1998; 397:60–68. [PubMed: 9671279]

Vigh B, Manzano e Silva MJ, Frank CL, Vincze C, Czirok SJ, Szabo A, Lukats A, Szel A. The system of cerebrospinal fluid-contacting neurons. Its supposed role in the nonsynaptic signal transmission of the brain. Histology and Histopathology. 2004; 19:607–628. [PubMed: 15024719]

Vitalis T, Cases O, Engelkamp D, Verney C, Price DJ. Defects of tyrosine hydroxylase-immunoreactive neurons in the brains of mice lacking the transcription factor Pax6. Journal of Neuroscience. 2000; 20:6501–6516. [PubMed: 10964956]

White JH, McIllhinney RAJ, Wise A, Ciruela F, Chan WY, Emson PC, Billinton A, Marshall FH. The $GABA_B$ receptor interacts directly with the related transcription factors CREB2 and ATFx. Proc Natl Acad Sci U S A. 2000; 97:13967–13972. [PubMed: 11087824]

Wullimann MF, Rink E. Detailed immunohistology of Pax6 protein and tyrosine hydroxylase in the early zebrafish brain suggests role of Pax6 gene in development of dopaminergic diencephalic neurons. Developmental Brain Research. 2001; 131:173–191. [PubMed: 11718849]

Wullimann MF, Rink E, Vernier P, Schlosser G. Secondary neurogenesis in the brain of the African clawed frog, *Xenopus laevis*, as revealed by PCNA, *Delta-1*, *Neurogenin-related-1*, and *NeuroD* expression. Journal of Comparative Neurology. 2005; 489:387–402. [PubMed: 16025451]

Xia Z, Dudek H, Miranti CK, Greenberg ME. Calcium influx via the NMDA receptor induces immediate early gene transcription by a MAP kinase/ERK-dependent mechanism. Journal of Neuroscience. 1996; 16:5425–5436. [PubMed: 8757255]

Zetterstrom RH, Williams R, Perlmann T, Olson L. Cellular expression of the immediate early transcription factors Nurr1 and NGFI-B suggests a gene regulatory role in several brain regions including the nigrostriatal dopamine system. Molecular Brain Research. 1996; 41:111–120. [PubMed: 8883941]

Zetterstrom RH, Solomin L, Jansson L, Hoffer BJ, Olson L, Perlmann T. Dopamine neuron agenesis in Nurr1−deficient mice. Science. 1997; 276:248–250. [PubMed: 9092472]

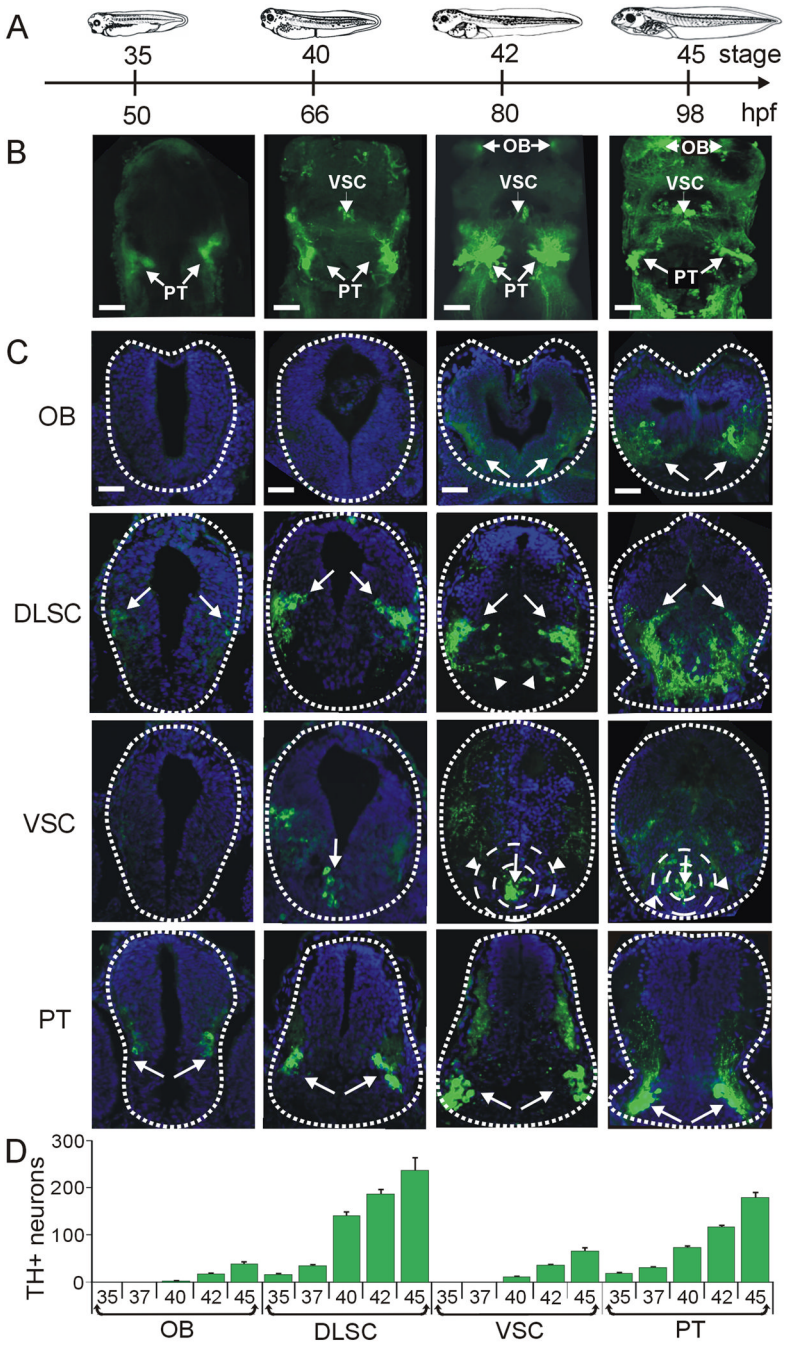

Figure 1. Development of brain dopaminergic nuclei

A. Developmental timeline showing stages and corresponding hr post fertilization (hpf) at which larvae were fixed for the images shown below. **B.** Wholemount projections of brains stained for TH show caudal to rostral appearance of dopaminergic nuclei. Images are ventral side and rostral end up. The PT nucleus is visible from stage 35; by stage 40 the VSC can be detected; by stage 42 the OB is also present. **C.** Cross sections through the brain were used for quantification of TH+ cells. TH staining is shown in green and DAPI staining of cell nuclei is shown in blue. Arrows point to TH+ cells in each section. The first row shows the olfactory bulb (OB), the second row shows the dorsolateral suprachiasmatic nucleus (DLSC). Arrowheads in this row point to a medial branch of the DLSC that becomes more

prominent during development. The third row depicts the ventral suprachiasmatic nucleus (VSC). The arrows point to the core and the arrowheads to TH+ cells in the annular region of the VSC, present from stage 42. The fourth row shows the PT nuclei. **D.** Quantification of the number of TH+ neurons per nucleus during development. Scale bars in B and C are 50 μm. Values are mean ± SEM for n≥6 larvae per stage.

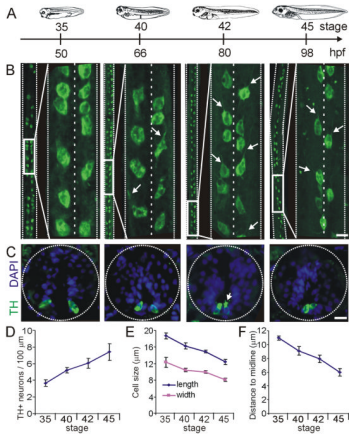

Figure 2. Development of spinal cord dopaminergic neurons

A. Developmental timeline as in Fig. 1. **B.** Wholemount projections of spinal cords stained for TH immunoreactivity. At each stage, large midbody segments of spinal cord are shown on the left side and an inset expansion is shown on the right. Projections are shown ventral side and rostral end up. Arrows on the stage 40, 42 and 45 panels point to axons extending rostrally. **C.** Cross sections through the spinal cord at different stages of development. Dopaminergic spinal neurons are located on the ventral side of the spinal cord. The arrow points to microvilli and cilia extending into the central canal. **D.** Quantification of the number of neurons per 100 µm of spinal cord at different stages of development. **E.** Length and width measurements of dopaminergic spinal neurons. **F.** Quantification of the distance to the midline. B,C, scale bars are 15 µm. Values are mean ± SEM for n≥4 larvae per stage.

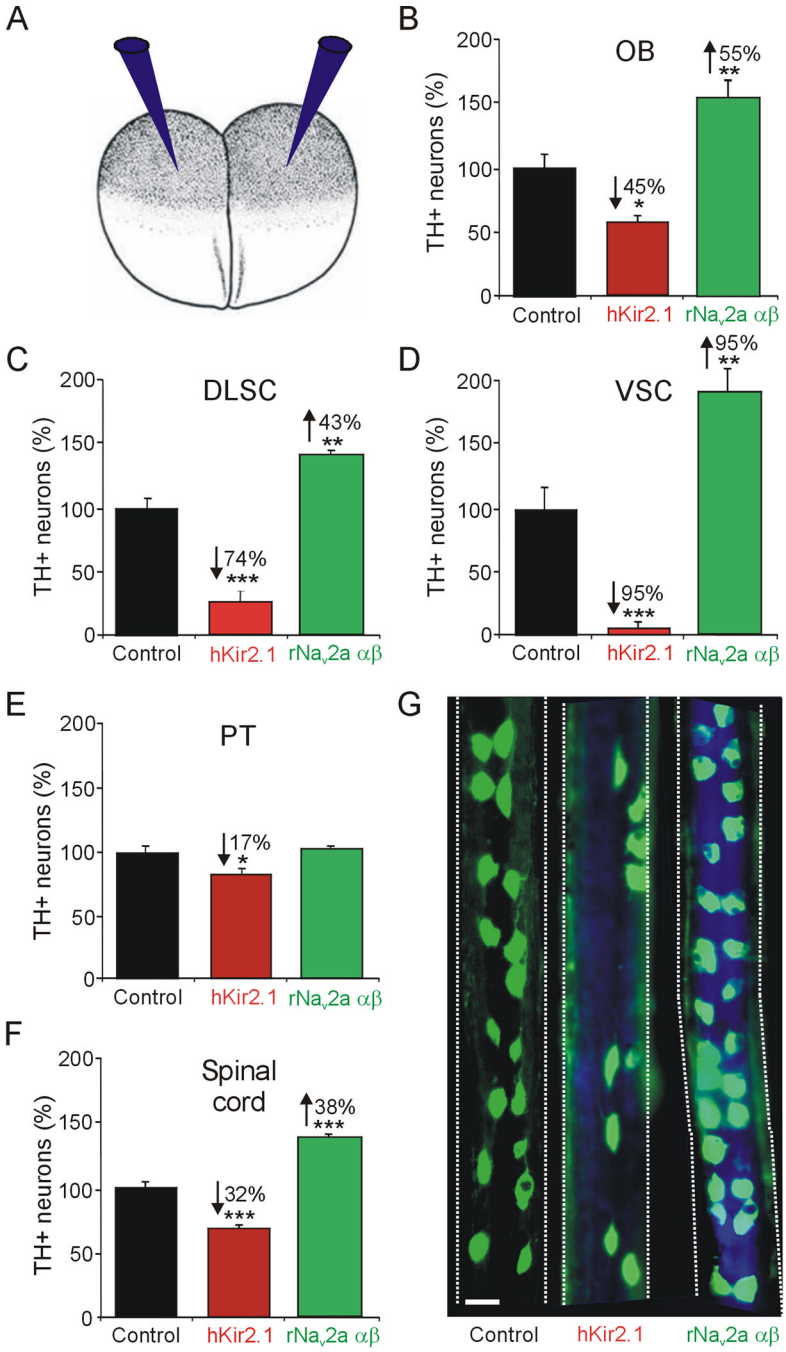

Figure 3. Dopaminergic specification is activity-dependent

A. Embryos at the two cell stage were injected bilaterally with either hKir2.1 or rNa$_v$2a αβ mRNA along with Cascade Blue tracer, to decrease or increase calcium spike activity, respectively (Borodinsky et al, 2004; Dulcis & Spitzer, 2008). **B–F.** Number of TH+ neurons (%) in activity-manipulated embryos in the OB (**B**), DLSC (**C**), VSC (**D**), PT (**E**) and spinal cord (**F**). **G.** Spinal cord wholemounts from stage 42 larvae stained for TH immunoreactivity (in green) show the effect of channel misexpression. The tracer (in blue) is seen in spinal cords from activity-manipulated larvae. Numerical percent change is indicated in cases of significant difference, marked by asterisks (n≥6 larvae per stage; values are mean ± SEM. *p<0.05, **p<0.01, ***p<0.001, comparing control values to hKir2.1 or

rNa$_v$2a αβ. The Mann Whitney U test was used to assess statistical significance). B, scale bar is 25 μm.

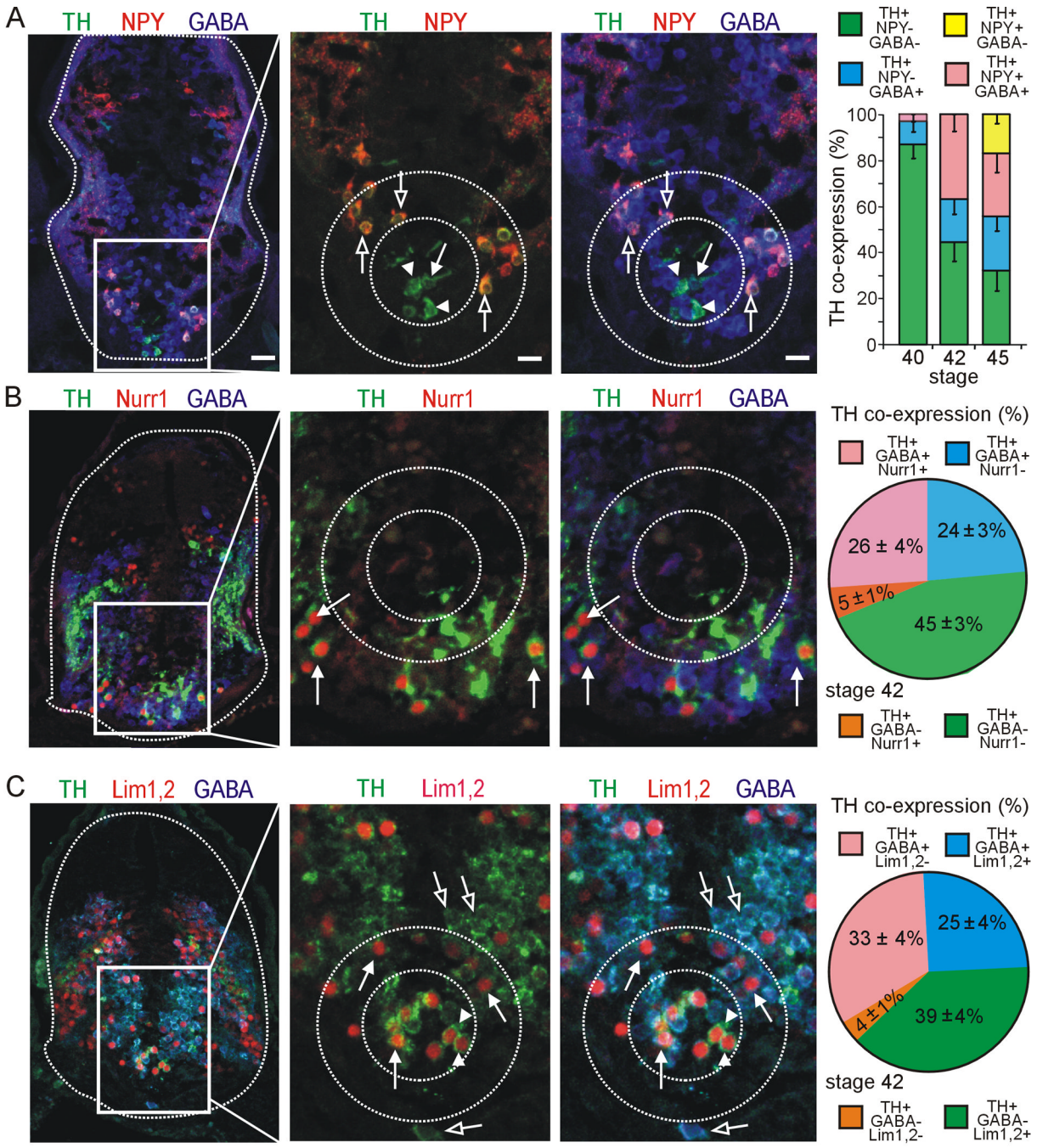

Figure 4. Co-expression of TH with other molecular markers during development of the VSC

GABA, NPY, or GABA/NPY are co-expressed in distinct regions of the VSC during development. **A.** Some TH+ cells in the core region (inner dashed circle) co-express GABA (arrow) while others are GABA− (arrowheads). TH+ neurons in the annular region are TH+/GABA+/NPY+ (outer dashed circle, open arrows). Graph shows developmental changes in proportions of GABA and NPY co-expression with TH. **B.** TH+ cells of the outer annular region co-express GABA and Nurr1 (arrows). This brain section depicts a more caudal region of the VSC. Graph shows the proportion of TH co-expression with GABA and Nurr1. **C.** TH+ cells of the core all co-express Lim1,2 (arrowheads), but some are also GABA+ (arrows), while the TH+ cells in the annulus co-express Lim1,2 and GABA (arrows). Cells

in the outer annular region are Lim1,2− but co-express TH and GABA (open arrows). Graph shows the proportion of TH co-expression with GABA and Lim1,2. A–C. Images are from stage 42 larvae. Scale bars in A apply to all figures in each column and are 80 μm for the first column and 40 μm for the second and third columns. Values are mean ± SEM for N≥4 larvae per stage.

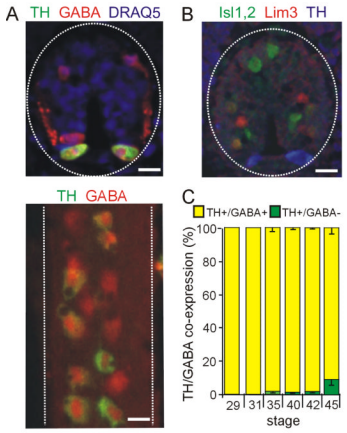

Figure 5. Co-expression of TH with GABA during development of the spinal cord

A. Upper panel: cross section through a stage 35 spinal cord shows co-expression of GABA in ventrally located dopaminergic cells. Dorsal GABAergic interneurons are also evident. Ventral side is down. Lower panel: wholemount of the spinal cord shows dopaminergic neurons within the rows of GABAergic ventral neurons in a stage 42 spinal cord. Ventral side is shown. **B.** TH does not co-localize with Lim3 or Isl1,2; stage 35 spinal cord. **C.** Percent co-expression of TH and GABA during development. Scale bars are 15 μm. Values are mean ± SEM for N≥4 late tailbud embryos or larvae per stage.

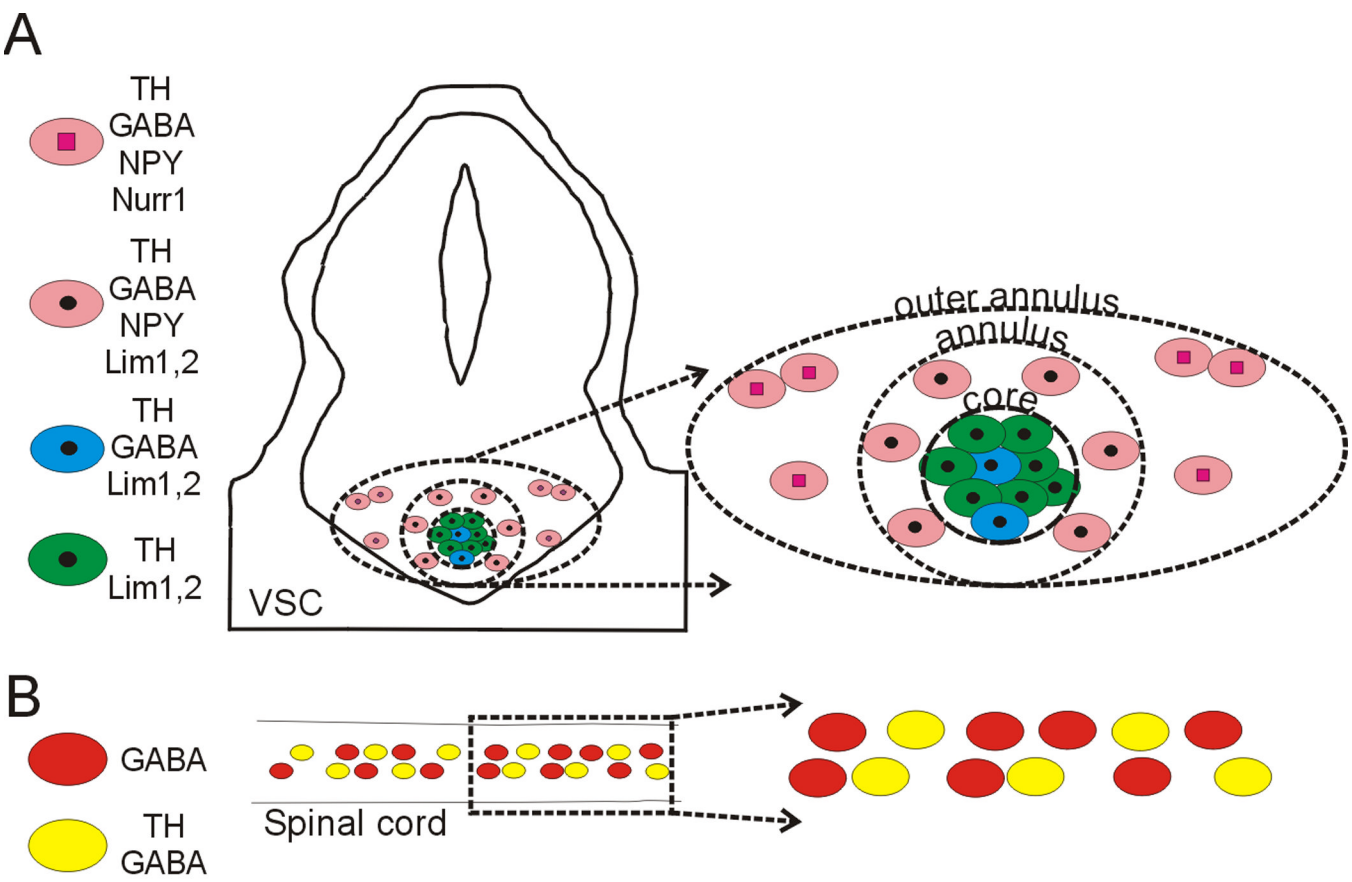

Figure 6. Subclasses of VSC and spinal cord dopaminergic neurons

The VSC is composed of four subclasses of dopaminergic neurons that can be identified by their co-expression of Lim1,2 or Nurr1 transcription factors and NPY and GABA neurotransmitters at stage 42. Spinal cord dopaminergic neurons constitute a single class at this stage. Panels on the right show expanded views of regions at the left.

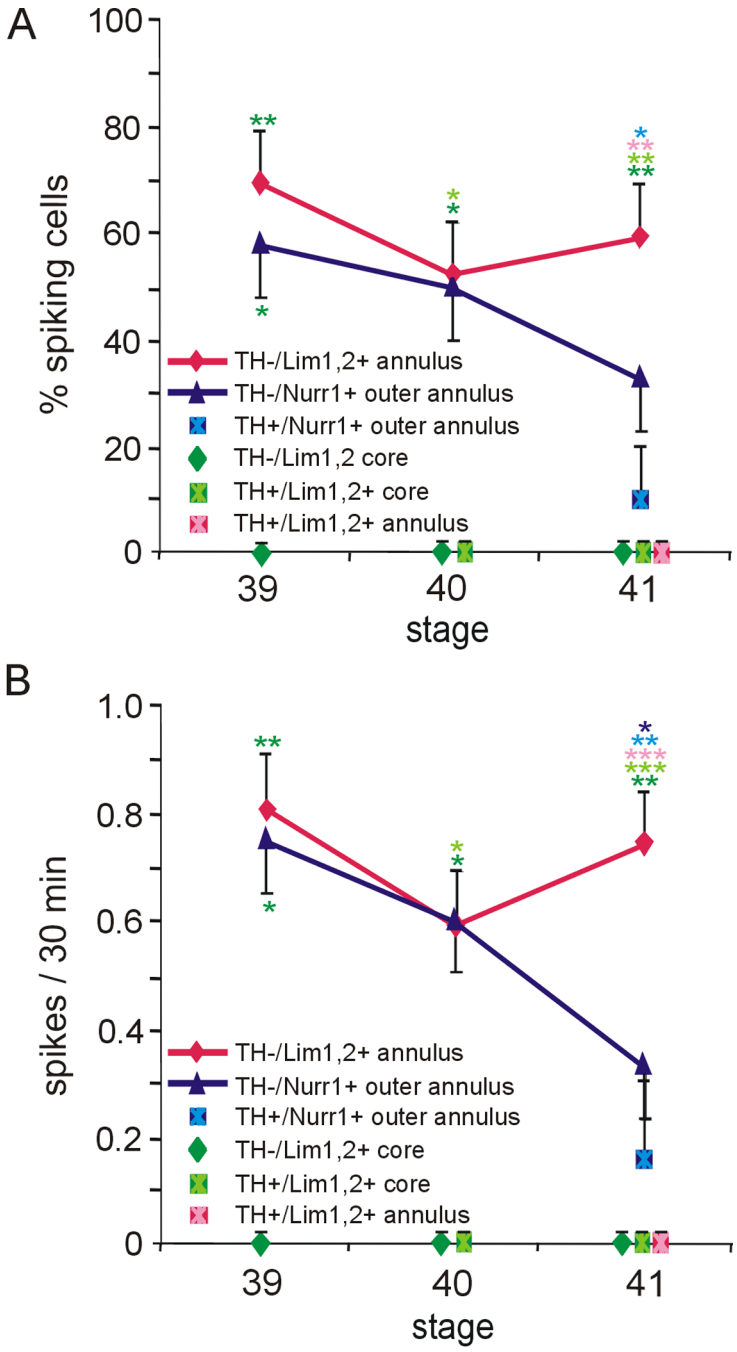

Figure 7. Spontaneous calcium spike activity in the VSC during TH acquisition

A. The incidence of spiking is different in VSC neurons expressing distinct molecular markers or located in different regions. Spikes were not detected in Lim1,2+ core and TH+/Lim1,2+ core neurons at stages 39–41, while spikes were initially observed in TH−/Lim1,2+ and TH−/Nurr1+ annular and outer annular neurons. At stage 41 spikes were not observed in annular TH+/Lim1,2+ neurons, although still recorded in some TH+/Nurr1+ outer annular neurons. **B.** The frequency of spiking is also different. TH−/Lim1,2+ and TH−/Nurr1+ annular and outer annular neurons initially have a similar frequency of spiking that diverges during development. By stage 41 annular TH+/Nurr1+ cells spike at a relatively low frequency, annular TH−/ Lim1,2+ cells spike at a relatively high frequency and spikes were

not observed in TH+/Lim1,2+ annular cells (n≥4 brain sections per stage with n≥4 neurons per class across brain sections; values are mean ± SEM. Asterisks indicate significant differences between cell types, color coded according to the figure labels. *p<0.05, **p<0.01, ***p<0.001; comparing across DA subtypes and across stages. The Kruskal-Wallis test followed by Conover post-hoc analysis was used to determine statistical significance).

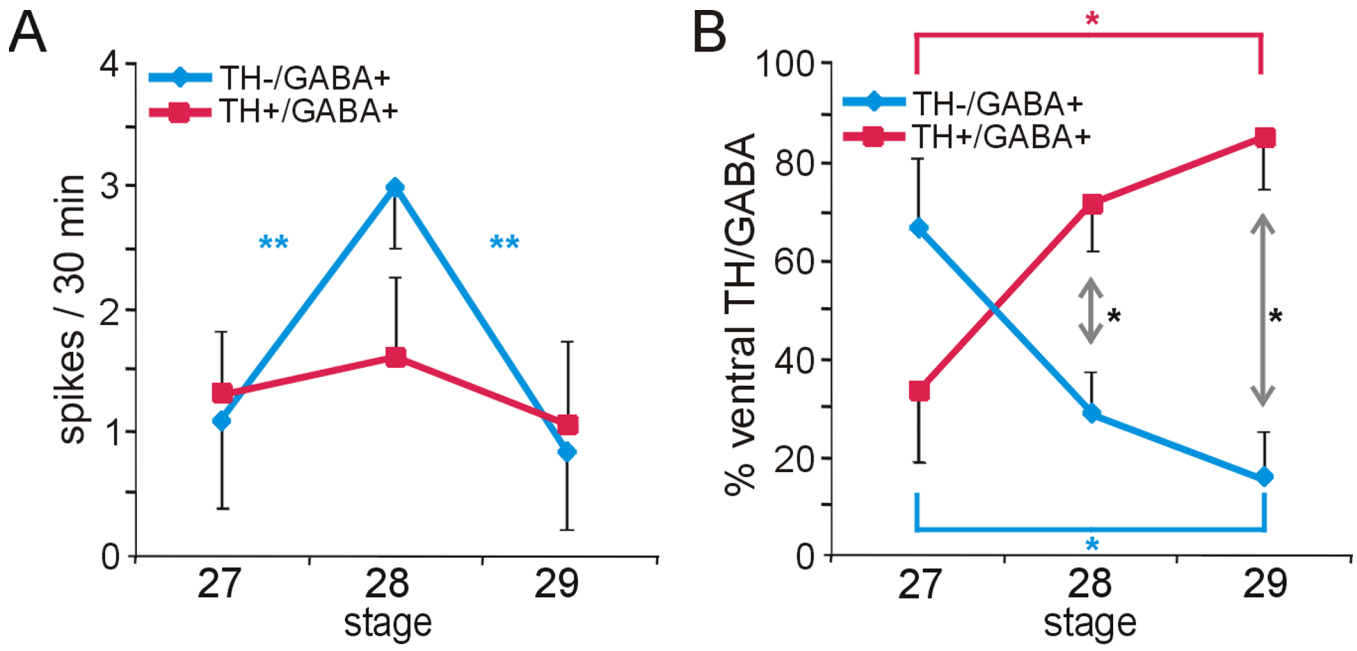

Figure 8. Spontaneous calcium spike activity and neurotransmitter expression in the spinal cord during TH acquisition

A. The incidence of calcium spiking is constant in spinal cord neurons at stages 27–29 (data not shown), but the frequency varies during this period: TH+/GABA+ neurons display a low and constant frequency of calcium spikes, while the TH−/GABA+ population shows an increase in frequency at stage 28 that decreases again by stage 29 (**$p<0.01$, comparing across stages; the Kruskal-Wallis test followed by Conover post-hoc analysis was used to determine statistical significance). **B.** The proportion of cells within the GABA immunoreactive population of the ventral spinal cord that are TH−/GABA+ and TH+/GABA+ changes during development, with the first group decreasing and the second increasing between stages 27, 28 and 29/30. Asterisks indicate significant differences between the TH−/GABA+ and TH+/GABA+ populations by stage (black asterisks; *$p<0.05$ assessed by the Mann-Whitney U test) and across developmental stages for each cell population (colored asterisks; *$p<0.05$ assessed by the Kruskal-Wallis test followed by Conover post-hoc analysis). ($n\geq4$ neural tubes with $n\geq7$ TH−/GABA+ or TH+/GABA+ neurons per neural tube per stage; values are mean ± SEM).

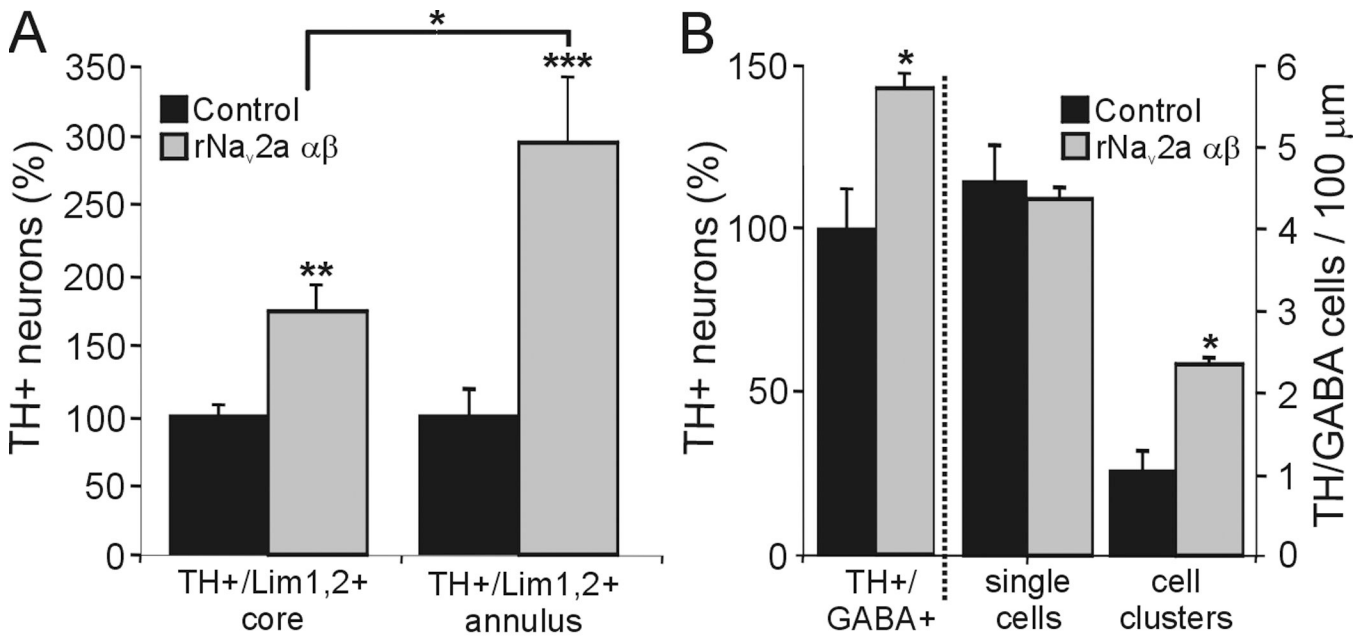

Figure 9. Neurotransmitter expansion in the VSC and spinal cord of activity-manipulated larvae

A. The number of TH neurons in the VSC core and annulus increases upon overexpression of rNa$_v$2a αβ. Expansion of the TH phenotype occurs within the Lim1,2 population in both core and annulus (**p<0.01, ***p<0.001, compared to control by the Mann-Whitney U test), and the expansion in the annulus is significantly greater than the expansion in the core (*p<0.05, comparing normalized control to rNa$_v$2a αβ values for the core and annulus with the Kruskal-Wallis test followed by the Conover post-hoc analysis). Stage 42; values are mean ± SEM for n=6 embryos. **B.** rNa$_v$2a αβ overexpression expands the TH phenotype within the ventral GABA+ population of the spinal cord (*p<0.05, comparing control versus rNa$_v$2a αβ values by the Mann-Whitney U test), increasing the number of clusters of TH+/GABA+ cells (*p<0.05, comparing control versus rNa$_v$2a αβ values by the Mann-Whitney U test). Stage 35; values are mean ± SEM for n≥4 larvae.

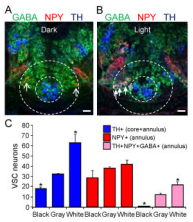

Figure 10. TH specification of NPY+/GABA+ VSC annular neurons following light adaptation

A. The VSC of a larva dark adapted on a black background for 2 hr and triple stained for TH, NPY and GABA is shown in a merged image of a transverse section. Arrows indicate TH−/NPY+/GABA+ neurons before induction of TH. **B.** The VSC of a larva light adapted on a white background for 2 hr and triple stained for TH, NPY and GABA in a merged image. Arrows indicate TH+/NPY+/GABA+ neurons following TH induction. A,B. Stage 42. Scale bars are 30 μm. C. Quantification of the number of neurons in the VSC that express TH, NPY, or TH+/NPY+/GABA+. Exposure to light increases and dark decreases the number of TH+ neurons recruited from the NPY+/GABA+ annular pool (n=6 larvae; values are mean ± SEM. *p<0.05 comparing light or dark conditions with low illumination on a gray background using the Mann-Whitney U test).